Nucleation and Growth of Oriented Ceramic Films onto Organic Interfaces

B. J. Tarasevich,* P. C. Rieke, and J. Liu

Battelle Pacific Northwest Laboratory, Richland, Washington 99352

Received August 17, 1994. Revised Manuscript Received September 27, 1995[⊗]

New materials synthetic methods are being investigated involving heterogeneous nucleation and growth of ceramic films from aqueous solutions onto surfaces modified with organic functional groups. Dense, nanocrystalline, iron hydroxide films were deposited onto sulfonated polystyrene and sulfonated self-assembling monolayers on oxidized silicon. (020) oriented goethite films were formed resulting in chains of edge-shared octahedra in the [001] direction lying parallel to the surface. Deposition amounts varied with pH primarily due to changes in solution supersaturation. The best films were formed when deposition occurred heterogeneously at supersaturations just below the critical supersaturation. Induction times decreased with increasing sulfonate site density due to a reduction in interfacial energy. Nucleation was initiated by binding of cationic species to sulfonate sites and hydrolysis and condensation reactions resulted in the growth and coalescence of crystallites.

Introduction

There has been recent interest in the use of two-dimensional organic interfaces containing specific functional groups to cause and control the nucleation of minerals from solution. Most of the studies have used surfaces containing acidic functional groups to study biomineralization processes. For example, calcium carbonate crystals were grown onto sulfonated polystyrene substrates[1] and Langmuir monolayers at the air−water interface.[2] Functional groups were chosen to model "nucleating" macromolecules thought to control calcium carbonate precipitation in mollusk shells.[3]

Acidic macromolecules in mollusks are primarily glycoproteins composed of protein regions with high concentrations of aspartic acid residues (containing carboxylic acid groups)[4] and sulfated polysaccharide regions[5] connected to the protein core. The glycoproteins are attached to the underlying silk−fibroin sheets in extracellular tissue regions. Heterogeneous nucleation is initiated from supersaturated solution by calcium binding onto acidic functional groups.[6,7] Proteins adopt the crystalline β-sheet conformation upon adsorption and it has been suggested that the β-sheets act as templates for oriented crystal growth due to specific spatial relationships between organic sites and calcium ions.[8,9] This results in mineral nucleation from specific lattice planes and interfacial control over crystallite orientation and polymorph. Similar degrees of control were suggested in the crystal growth studies on model organic interfaces as the functional group type and structure affected the calcium carbonate nucleation density, orientation, and polymorph.

Recent work has involved the use of Langmuir monolayers as nucleating templates for the solution formation of materials of technological interest such as oriented barium sulfate[10] and nanosized cadmium sulfide particles.[11] This work suggested that organic monolayers can be used to engineer crystals with specific orientations and crystallite sizes. There has been little previous work, however, on the growth of continuous ceramic thin films onto self-supported substrates modified with organic functional groups.[12]

We report the solution nucleation and growth of thin films of iron hydroxides onto sulfonated polystyrene substrates and sulfonated self-assembling monolayers attached to oxidized silicon. Instead of calcium carbonate, we are interested in using organic interfaces to deposit materials that have applications as optical, magnetic, or protective materials. Organic molecules were covalently attached to rigid substrates to form interfaces more chemically and structurally stable than Langmuir monolayers and, therefore, more practical. Iron hydroxides were chosen because they are common biominerals and because they have applications as catalysts and ion exchangers and are precursors to magnetic phases which are important in magnetic storage devices.

The goals of this work are 2-fold: (1) to demonstrate that an approach involving organic interfaces can be used to synthesize ceramic films and (2) to determine some of the important issues involved in thin-film nucleation and growth processes. Thin films of iron hydroxides were deposited onto modified surfaces, and

[⊗] Abstract published in *Advance ACS Abstracts,* November 1, 1995.

(1) Addadi, L.; Moradian, J.; Shay, E.; Maroudas, N. G.; Weiner, S. *Proc. Natl. Acad. Sci. U.S.A.* **1987**, *84*, 2732.
(2) (a) Rajam, S.; Heywood, B. R.; Walker, J. B. A.; Mann, S.; Davey, R. J.; Birchall, J. D. *J. Chem. Soc., Faraday Trans.* **1991**, *87*(5), 727. (b) Heywood, B. R.; Rajam, S.; Mann, S. *J. Chem. Soc., Faraday Trans.* **1991**, *87*(5), 735. (c) Heywood, B. R.; Mann. S. *Chem. Mater.* **1994**, *6*, 311.
(3) Weiner, S. *CRC Crit. Rev. Biochem.* **1986**, *20*, 365.
(4) Weiner, S. *J. Chromatogr.* **1982**, *245*, 148.
(5) Greenfield, E. M.; Wilson, D. C.; Crenshaw, M. A. *Am. Zool.* **1984**, *24*, 925.
(6) Worms, D.; Weiner, S. *J. Exp. Zool.* **1986**, *237*, 11.
(7) Crenshaw, M. A.; Ristedt, H. In *The Mechanisms of Mineralization in the Invertebrates and Plants*; Watabe, N., Wilber, K. M., Eds.; University of S. Carolina Press: SC, 1974; p 355.
(8) Weiner, S.; Traub, W. *Philos. Trans. R. Soc. London B* **1984**, *304*, 425.
(9) Mann, S. *Nature* **1988**, *332*, 119.
(10) Heywood, B. R.; Mann, S. *Langmuir* **1992**, *8*, 1492.
(11) (a) Yi, K. C.; Fendler, J. H. *Langmuir* **1990**, *6*, 1519. (b) Zhao, X.; Xu, S.; Fendler, J. H. *Langmuir* **1991**, *7*, 520.
(12) Tarasevich, B. J.; Rieke, P. C. *MRS Symp. Proc.* **1990**, *174*, 51.

0897-4756/96/2808-0292$12.00/0

properties such as morphology, orientation, and phase were examined. In addition, the effects of solution chemistry and surface site density on deposition were studied.

Experimental Procedure

Surface Modification and Analysis. Polystyrene surfaces were obtained as substrates cut from petri dishes or were formed as thin films by dip-coating glass slides into solutions of polystyrene dissolved in xylene. Cast thin films were heat treated at 100 °C for 12 h. Sulfonate groups were attached to the polystyrene surfaces by reaction in concentrated sulfuric acid solutions for various time periods. Surfaces with higher sulfonate concentrations were prepared for infrared spectroscopy experiments by reactions with sulfur trioxide vapor in a two-stage reactor. The reactor was placed under low vacuum, sulfur trioxide vapor was introduced for various time periods, and the reactor was purged. Samples were washed thoroughly, dried, and stored under nitrogen.

Sulfonated self-assembling monolayers (SAMs) were prepared as follows. Silicon wafers were cleaned in chloroform and in an air plasma. Surfaces were washed in 0.1 M KOH, 0.1 M HNO_3, and water. Monolayers were formed by placing wafers into solutions of vinyl-terminated alkyl (C_{17}) trichlorosilanes in cyclohexane. The vinyl group was converted to a sulfonate group by reaction in sulfur trioxide vapor.

X-ray Photoelectron Spectroscopy (XPS). Electron binding energies of modified surfaces were obtained on a Perkin-Elmer 560 spectrometer using Mg Kα radiation at 1253.6 eV. Survey scans were obtained from 0 to 975 eV using 100 eV pass energy, and multiplex spectra were obtained for carbon 1s, oxygen 1s, and sulfur 2p peaks using 25 eV pass energy. Peak positions were corrected for charging by assigning the carbon 1s peak to 285 eV. Peak heights or integrated areas were obtained and corrected using sensitivity factors of 0.49, 0.66, and 0.25 for sulfur 2p, oxygen 1s, and carbon 1s peaks, respectively. Intensities were used to calculate atomic ratios between elements. Estimates of fractional sulfonate coverage were obtained from C1s and S2p intensities by quantitative analyses described elsewhere.[13]

Contact Angle Measurements. Contact angles of aqueous buffer solutions onto sulfonated surfaces were obtained using a Raame-Haake contact angle goniometer. Samples were placed into a sealed environmental chamber maintained at 100% humidity by the presence of wetted sponges. Advancing contact angles of 0.002 mL drops of buffer solution were obtained. Standard buffer solutions were prepared for pH values ranging from 1.4 to 10.2.[14] Measurements were obtained within 30 s of drop placement, and at least eight measurements were obtained for each sample for drops placed randomly across the substrate surface.

Film Deposition and Characterization. *General Methods.* Solutions were formed with various salt anion types (iron(III) chloride or iron(III) nitrate), iron salt concentrations (1×10^{-4}–1×10^{-1} M) and pH values (adjusted by adding HNO_3, HCl, or NaOH) in 0.22 μm filtered, deionized water (18 MΩ cm resistivity). Solutions were prepared from refrigerated stock solutions or made fresh to prevent precipitation before use and were 0.22 μm filtered. pH measurements were made on an Orion Model 720A pH meter using a pH electrode and double junction reference electrode. Substrates were placed into a two-stage Teflon-coated reaction vessel equipped with a reflux condenser or polyethylene containers within a water bath. Polymer containers were used to avoid any silica dissolution that may occur at high pH values and temperatures and to prevent nucleation onto glass surfaces. The experimental solutions were placed into the reactor with the substrates at room temperature. The solution reactor or baths were heated to 40–100 °C ± 0.1 °C by a temperature controller and thermocouple placed in the solutions.

Characterization. Films phases were determined by powder X-ray diffraction of films removed from substrates on a Phillips diffractometer using Cu Kα radiation at 40 kV. Microstructures of thin film fracture edges were obtained using a Hitachi S-800 field emission scanning electron microscope (FEM) at 25 kV and 70–80° tilt. Films attached to silicon and polystyrene substrates were embedded in epoxy resin. Samples were ultramicrotomed to form planar or cross sections of the films. Films were examined using a Phillips 400 transmission electron microscope (TEM) at 120 kV. Large-area diffraction of intact films and microdiffraction of individual crystallites was performed. An ISI-SX-40 scanning electron microscope was used to obtain planar views and an energy-dispersive X-ray spectrometer was used to obtain X-ray spectra of patterned films.

Speciation Calculations. Solution supersaturations were determined as a function of iron concentration, solution pH, and temperature for iron nitrate solutions using the EQ3NR program.[15] This program solves simultaneous equations for mass balance, charge balance, and chemical reactions. The speciation equations and reaction constants used were described previously.[16] Species concentrations were calculated, and supersaturation values were determined relative to various phases by obtaining activity products of species involved in precipitate formation divided by the respective solubility products in terms of activities. Activity coefficients were calculated by successive approximations using the B-dot equation. The B-dot equation was used because it was developed for use at a wide range of temperatures.[17]

Deposition Amounts. Deposition amounts were examined as a function of solution pH and surface site density. Sulfonated polystyrene samples were placed into solutions heated to 40–70 °C and were removed after various time periods. Amounts deposited were determined using UV–visible spectrophotometry and atomic absorption spectroscopy. UV–visible spectroscopy was used previously to characterize growth rates in sputtered iron oxide films[18] and precipitation of iron hydroxide particles.[19] Absorbances occurred from ~280 to 500 nm and were referenced to sulfonated polystyrene substrates. Deposits from known areas were dissolved from the substrates in concentrated nitric acid. Fe^{3+} concentrations were determined using atomic absorption spectroscopy and were converted to μg of Fe/cm^2. Plots of UV–visible absorbance at 300 nm versus μg/cm^2 from atomic absorption were linear. Once a standard curve was obtained relating UV–visible absorbance to mass, repetitions of the experiment were done using UV–visible absorbances only.

Results and Discussion

Surface Modification and Analysis. Sulfonation of polystyrene surfaces was evidenced by attenuated total reflectance FTIR and XPS analysis. Infrared spectra showed asymmetric SO_3– stretching peaks in the 1200 cm^{-1} region (~1214 and 1179 cm^{-1}) and a symmetric SO_3– stretching peak at 1041 cm^{-1}.[20] A peak at 831 cm^{-1} was assigned to out of plane bending of C–H groups adjacent to para-substituted benzene, indicating that sulfonate groups were in the para position.

Sulfonated SAMs on silicon were analyzed by ellipsometry, XPS, and contact angle wetting. XPS analysis

(13) Seah, M. P. In *Practical Surface Analysis by Auger and X-ray Photoelectron Spectroscopy*; Briggs, D., Seah, M. P., Eds.; John Wiley & Sons: New York, 1983; p 181.

(14) Robinson, R. A.; Stokes, R. H. *Electrolyte Solutions*; Butterworth: London, 1959.

(15) Wolery, T. J.; EQ3NR–A Computer Program for Geochemical Aqueous Speciation–Solubility Calculations, UCRL-MA-110662 pt. III, Lawrence Livermore National Lab, 1992.

(16) Rieke, P. C.; Marsh, B. D.; Wood, L. L.; Tarasevich, B. J.; Liu, J.; Song, L.; Fryxell, G. E. *Langmuir* **1995**, *11*, 318.

(17) Helgeson, H. C. *Am. J. Sci.* **1969**, *267*, 729.

(18) Morl, K.; Ropke, U.; Knappe, B.; Lehmann, J.; Perthel, R.; Schroder, H. *Thin Solid Films* **1979**, *60*, 49.

(19) Dousma, J.; deBruyn, P. L. *J. Colloid Interface Sci.* **1976**, *56*, 527.

(20) Levy, L. Y.; Jenard, A.; Hurwitz, H. D. *J. Chem. Soc., Faraday Trans.* **1980**, *76*, 2558.

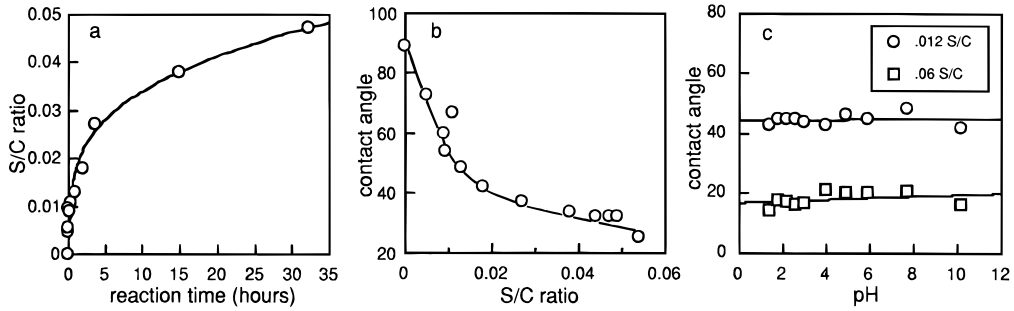

Figure 1. (a) S/C ratio as a function of reaction time in sulfuric acid, (b) S/C ratio versus contact angle (pH 7.7 buffer solution), and (c) contact angles as a function of buffer solution pH for substrates at low and high sulfonate coverage.

indicated the presence of carbon and sulfur. Monolayer thicknesses were 25 Å, and contact angles were less than 15°. These analyses indicated the formation of dense monolayers terminated by sulfonate groups.

Sulfonate coverages on polystyrene could be varied as a function of reaction time in sulfuric acid as indicated by XPS data in Figure 1a. There is an initial region of fast sulfonation and second region of slower sulfonation. The second region above 0.03−0.04 S/C corresponds to attainment of complete surface coverage and start of subsurface sulfonation at substantially reduced rates. These S/C ratios are on the same order of magnitude as saturation coverage S/C values determined by calculation (0.05 S/C) and by previous studies.[21] It is assumed that the sulfonate groups are randomly attached to the benzene rings as the reaction proceeds so that the average site spacing is inversely proportional to the sulfonate coverage. Since the intersite spacing of sodium naphthalene sulfonate molecules in crystalline Langmuir monolayers is 6 Å,[22] and intersite spacing of Langmuir monolayers of *n*-eicosyl sulfate is 5 Å,[2c] sulfonate intersite spacing on polystyrene approaches 5−6 Å at full coverage. The sites are arranged in a disordered structure on the surface since polystyrene is an amorphous polymer and benzene rings are disordered.

Figure 1b shows that the contact angle decreases with increasing S/C ratio. This indicates an increase in surface hydrophilicity which would be expected with increasing hydrogen-bonding interactions between water molecules and sulfonate sites in contrast to less attractive interactions between water molecules and less polar benzene and carbon chain molecules. The contact angles vary continuously from a pure polystyrene surface (90°) down to 25°, suggesting a continuous change in surface sulfonate coverage. Near saturation coverage of groups was obtained as indicated by the ∼20−25° minimum contact angle.

The kinetics of polystyrene sulfonation from the vapor phase were much faster than sulfuric acid sulfonation resulting in full coverage in less than 1 min reaction time. It was not possible to prepare surfaces with various coverages by this method. Maximum S/C ratios were 0.074 and contact angles were nearly 0°, suggesting full coverage. Coverage estimates, however, were greater than 1, indicating that sulfonate groups were located in the subsurface regions. SEM examination showed the presence of grooves and microcracks suggesting some etching into the subsurface.

Figure 1c shows data for contact angles as a function of buffer solution pH for surfaces at high and low sulfonate coverages (0.06 and 0.012 S/C ratio). The data indicate that the contact angle values do not change significantly between pH values of 1.4 and 10.2. Contact angle changes with pH have been found to correspond to the p*K* of ionization of carboxylated and aminated surfaces.[23] Figure 1c shows that sulfonate sites are ionized at all pH values examined and that the p*K* value is less than 1.4. This is consistent with the expected high acidity of benzene sulfonate groups and p*K* values of less than 1.0 for sulfonated ion-exchange resins.[24] This indicates that the sulfonate group surface chemistry is independent of pH and does not complicate the interpretation of nucleation and growth studies at various pH values.

Deposition Studies. The thermodynamic conditions required for nucleation and growth from solution have been described by classical nucleation theory[25] and result in an activation energy for formation of a critical nucleus of radius *r** of

$$\Delta G^* = \frac{16\pi(\sigma)^3}{3(pRT \ln S/M)^2} \qquad (1)$$

where σ is the interfacial tension, S is the supersaturation, p is the precipitate density, and M is the molecular weight. This expression indicates that the activation energy can be decreased and nucleation promoted by increasing the solution supersaturation or by decreasing the interfacial energy. In our studies, the supersaturation was varied by varying the solution temperature and pH and the interfacial energy was controlled by varying the surface site density.

Effect of pH on Deposition Amounts. The role of supersaturation on nucleation and growth was examined by varying solution conditions such as pH. Figure 2a shows amounts deposited onto full coverage sulfonated polystyrene after 6 hours from 2×10^{-3} M iron nitrate solutions at 70 °C as a function of pH. Solutions were monitored for the onset of homogeneous nucleation by observations of scattering by a helium−neon laser and by particle size analysis using a MicroTrac Series 9200 particle size analyzer. Strictly, any precipitation in solution may occur by heterogeneous nucleation onto

(21) Bigelow, R. W.; Bailey, F. C.; Salaneck, W. R.; Pochan, J. M.; Pochan, D. F.; Thomas, H. R.; Gibson, H. W. *Adv. Chem. Ser.* **1980**, *187*, 295.
(22) Vogel, V.; Mullin, C. S.; Shen, Y. R. *Langmuir* **1991**, *7*, 1222.
(23) Holmes-Farley, S. R.; Reamey, R. H.; McCarthy, T. J.; Deutch, J.; Whitesides, G. M. *Langmuir* **1985**, *1*, 725.
(24) Helfferich, F. G. *Ion Exchange*; McGraw-Hill: New York, 1962; p 86.
(25) Mullin, J. W. *Crystallization*; Butterworth: London, 1972.

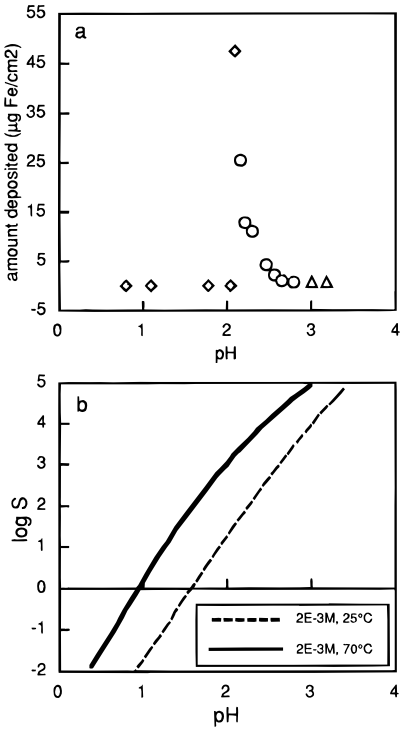

Figure 2. (a) Deposition amounts as a function of pH from 2 × 10^{-3} M 70 °C iron nitrate solutions after 6 h: (◊) no solution precipitation, (○) solution precipitation occurred between 0.5 and 6 h, (△) solution precipitation occurred at $t = 0$; (b) calculated supersaturation values versus pH for 2 × 10^{-3} M iron nitrate solutions at 25 and 70 °C with respect to goethite.

impurities as well as homogeneous nucleation. Therefore, we will use the term "solution precipitation" to describe particle formation in solution. Usually, precipitation corresponded to an orange-red tinting of the solutions. Solutions that had solution precipitation are noted by symbols corresponding to the time of the onset of precipitation.

Figure 2a indicates that the amounts deposited after 6 h were highly pH dependent, and high deposition amounts occurred over a very narrow pH range. No deposition occurred at low pH values until pH 2.10 was reached. This solution resulted in the highest deposition amount after 6 h. The subsequent decrease in deposition amounts with pH correlated to the occurrence of solution precipitation.

The results are best explained by changes in supersaturation with pH. Figure 2b shows log supersaturation versus pH for the 2 × 10^{-3} M solutions at 25° and 70°. For log $S > 0$, solutions were supersaturated and for log $S < 0$, solutions were undersaturated. Supersaturation values were calculated with respect to goethite because this was the only phase formed under the solution conditions used. Figure 2b indicates that the initial acidic solutions (pH 1−2) were undersaturated or at low supersaturation at 25 °C. Increasing the solution temperature to 70 °C resulted in increasing the supersaturation. The supersaturation is strongly affected by solution pH, increasing sharply with increasing pH. Most of the work described here involved deposition from heated acidic solutions because it was easier to control S by increasing the solution temperature than by adding base which resulted in sharp increases in S and local precipitation due to inhomogeneous mixing.

There was no deposition for the pH 1.1 through pH 2.0 solutions even though these solutions were supersaturated with respect to goethite. Deposition did occur at later times for the pH 2.0 solution (between 6 and 18 h), indicating a longer induction time was required for nucleation. The induction time is the time required to form critical nuclei before growth. Significant deposition occurred for solutions at pH 2.1 after an induction period of ∼2 h. Although there is only a small pH change from pH 2.0, the supersaturation increased from 1202 to 1660. Deposition occurred heterogeneously since there was no solution precipitation.

The supersaturation was 2512 for the pH 2.17 solution. It appeared that the induction time was shorter (∼1 h) and the rate of deposition higher than for the pH 2.1 solution as would be expected from the higher supersaturation. Growth slowed earlier, however, because solution precipitation occurred (at ∼4 h) and lowered S, depleting species available for heterogeneous growth. This resulted in lower final amounts deposited. Similar trends occurred for the pH 2.23−2.57 solutions with the induction times for heterogeneous nucleation and solution precipitation decreasing with increasing pH. In all cases, heterogeneous nucleation occurred first, as would be expected by the lower free energy. These solutions are close to the critical supersaturation which is an empirically determined supersaturation value at which solution precipitation dominates. Even though precipitation occurred in solution at later time periods, good high-density films were formed heterogeneously. These conditions may be advantageous for processing in that the deposition rates were faster than deposition from the pH 2.1 solution.

Based was added to obtain solutions with pH values greater than 3. Extensive solution precipitation occurred for these solutions upon addition of base as would be expected by the high supersaturation values predicted. These solutions were at or above the critical supersaturation. The deposition mechanism in these cases involved the adsorption of solution-formed colloidal particles onto the sulfonated surfaces. Iron hydroxide particles are positively charged at these pH values and can adsorb onto negatively charged surfaces by long-range electrostatic interactions. Very little material was deposited, and the amount corresponded to a 40 Å layer of iron hydroxide. This suggests the adsorption of a monolayer of nanosized particles. This is consistent with previous work on solution precipitation of goethite particles which found the initial formation of particles ∼40−60 Å in diameter.[26] Films formed by the adsorption of colloidal particles above pH 3 were not dense or continuous and not as well adhered to the substrate as films formed by heterogeneous nucleation.

Speciation calculations[16] and UV−visible spectroscopy indicated that the initial iron salt solutions consisted of primarily $FeOH^{2+}$ and Fe^{3+} species at 70 °C. UV−visible spectroscopy and XPS of deposited thin films showed no evidence for the presence of these unreacted species. UV−visible spectra of films did show absorbances which indicated the formation of condensed Fe−O−Fe or Fe−OH−Fe structures.[19] This indicates that the initial species present in solution reacted by hy-

(26) Dousma, J.; deBruyn, P. L. *J. Colloid Interface Sci.* **1978**, *64*, 154.

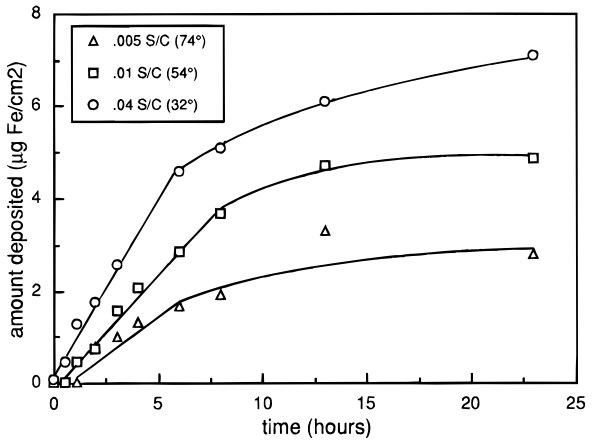

Figure 3. Deposition amounts over time from iron nitrate solutions at various sulfonate site densities.

drolysis and condensation reactions to form the deposited films.

Effect of Surface Sites on Deposition Kinetics. The role of the organic interface on nucleation and growth was examined by varying the surface site density. Figure 3 shows deposition data from pH 2.5, 1×10^{-2} M iron nitrate solutions at 40 °C onto surfaces with various sulfonate coverages. All substrates were placed into the same stirred solution and deposition resulted in supersaturation changes of less than 1.5% until solution precipitation occurred.

Figure 3 shows that there was no induction time for deposition at complete sulfonate coverage. Induction times occurred at lower sulfonate coverages and increased with decreasing coverage (0.5, 1 h) for 0.01 S/C (~25% coverage) and 0.005 S/C (~12% coverage), respectively. The kinetics of nucleation can be expressed by equations of the form

$$1/\tau = A \exp[-\Delta G^*_{\text{het}}/kT] \qquad (2)$$

where τ is the induction time and A is a constant. Similar expressions can be written in terms of N, the total number of nuclei formed, or I, the nucleation rate in terms of mass or number of nuclei per time. The expressions indicate that τ decreases or the nucleation rate increases with decreasing energy barrier for formation of critical nuclei, ΔG^*, given by eq 1. For our experiment, S is the same for all surfaces. According to classical theory, a reduction in τ can only occur if G^*_{het} decreases by decreasing the interfacial energy term, σ. A reduction in τ with sulfonate site density, therefore, indicates a decrease in interfacial energy with increasing sulfonate site density.

The film growth was initially linear with time followed by a nonlinear region of much lower growth rate. The nonlinear region was due to a reduction in supersaturation when solution precipitation occurred at later time periods and depleted species from solution. The nonlinear region could be shifted to later times by delaying the onset of solution precipitation using solutions with lower supersaturations.

The rate of growth (slope of the deposition curve) increased with increasing sulfonate density and decreasing induction time. We found that this trend was reproduced using other solution supersaturations. TEM microscopy showed that surfaces with higher sulfonate

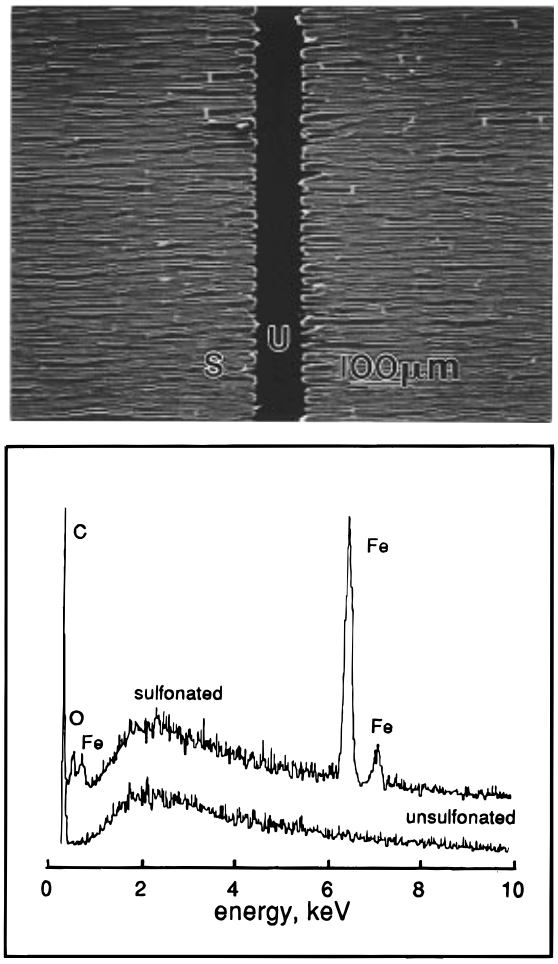

Figure 4. SEM picture of patterned film and X-ray spectra of unsulfonated (U) regions and sulfonated regions (S).

site densities had higher crystallite densities (smaller crystallite sizes) than surfaces with lower site densities. Classical nucleation and growth theory predicts that nucleation densities increase with decreasing interfacial energy. This suggests that growth rates reflect differences in numbers of nuclei formed, as overall growth rates equal the growth rate per nucleus times the number of nuclei. Calculations indicated that overall growth rates increase with crystallite density even after film coalescence if the deposition occurs by the lateral growth of iron hydroxide chains at constant growth rate per chain. Evidence for the chain morphology and layer-by-layer growth mechanism is discussed in detail later. This result deserves more attention beyond the scope of this work and will require more detailed deposition studies and microstructural evaluations to determine when film coalescence occurs and how growth rates are affected by crystallite size, density, and growth morphology.

An increase in sulfonate site density, therefore, resulted in a reduction in the induction time for nucleation, indicating a decrease in interfacial energy. Experiments have been carried out to obtain induction times for a larger range of surface site densities at various supersaturation values in order to experimentally determine interfacial energy values and confirm this trend.[27] The molecular-level interactions that affect

(27) Rieke, P. C.; Wiecek, R.; Marsh, B. D.; Wood, L. L.; Tarasevich, B. J.; Liu, L.; Song, L.; Fryxell, G. E., submitted to *Langmuir*.

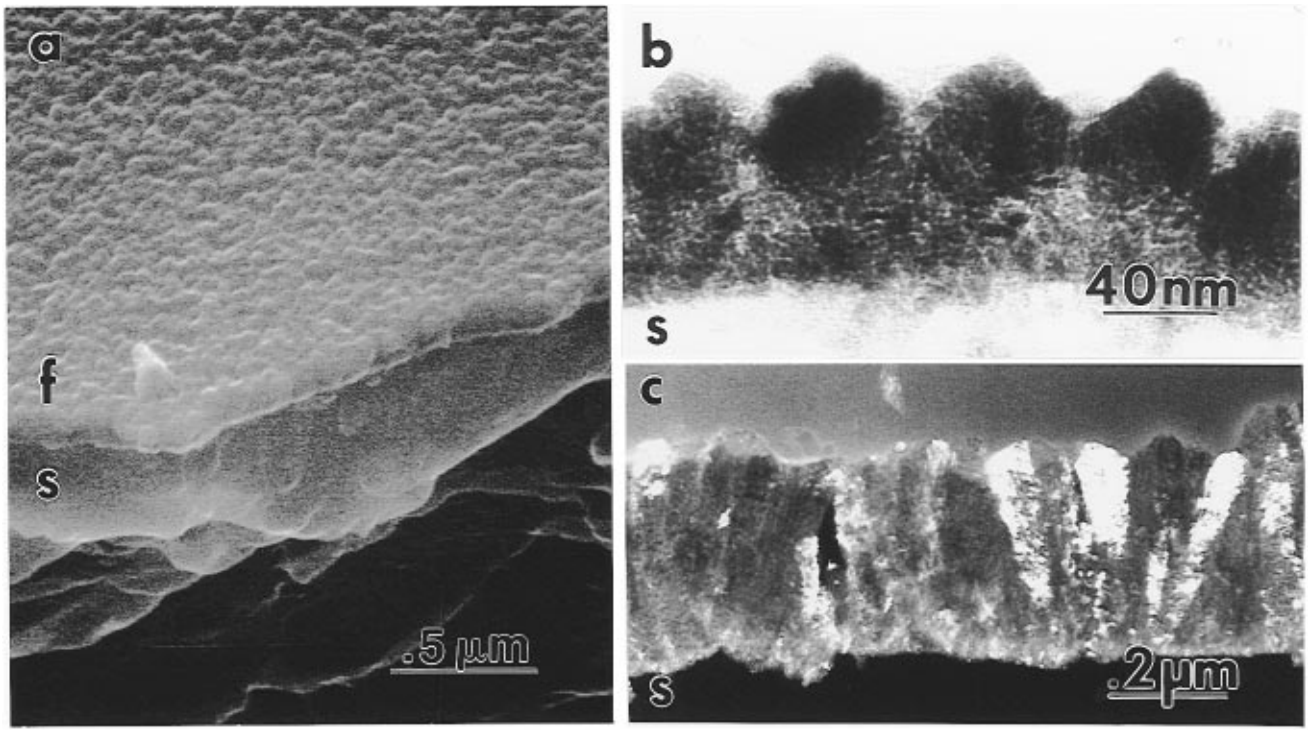

Figure 5. (a) FEM tilted view of fracture edge of goethite film on sulfonated polystyrene, (b) TEM cross section of akaganeite film on sulfonated polystyrene, and (c) TEM dark-field cross section of goethite film on sulfonated SAM on silicon; f, film; s, substrate.

the interfacial energy involve electrostatic binding interactions between solution species and sulfonate sites. XPS and FTIR experiments indicated that iron species adsorbed onto sulfonate sites soon after placement into solutions and that the amounts absorbed increased with sulfonate site density. An increase in nucleation rate, therefore, corresponds to a greater number of binding interactions between species and surface sites.

The role of sulfonate sites in promoting deposition was also demonstrated by deposition onto surfaces that were patterned to have sulfonated and unsulfonated regions. Figure 4 shows a micrograph of a film deposited onto a sulfonated polystyrene substrate that was patterned to form unsulfonated polystyrene bars alternating with sulfonated resions. The bars were formed by removing sulfonate sites with a scribe to expose underlying unsulfonated polystyrene, similar to techniques described previously for patterning thiol SAMs on gold.[28] Sulfonated substrates were patterned first and then placed into solutions for deposition. X-ray spectra of the unsulfonated and sulfonated regions is shown. The spectra indicate that iron and oxygen are found in the regions that contain sulfonate sites but only carbon is found in the unsulfonated bar regions. The carbon signal comes from the underlying polystyrene substrate and carbon coating. This indicates that deposition was confined to the sulfonated regions and not the unsulfonated regions. Selective deposition onto sulfonated regions is also indicated by contrast between lighter iron hydroxide regions and darker unsulfonated regions in the SEM micrograph. Part of the contrast is due to the depth of the bars (10−50 μm). There was some cracking of the film due to cracking of the underlying sulfonated substrate during heating. This occurred because the surface was highly sulfonated and had microcracks due to etching.

Clearly, the sulfonate sites have a significant effect in promoting the deposition of the iron hydroxide deposit compared to the unmodified surface. The ability to confine deposition to sulfonate regions and not unsulfonated regions over the entire deposition period, however, depended to a large extent on the solution chemistry conditions. For example, deposition occurred from the pH 2.1, 2×10^{-3} M iron nitrate solution in Figure 2 onto sulfonated surfaces but not unmodified surfaces after 6 h. These conditions resulted in the best localization of deposition for patterned surfaces in Figure 4 and for electron beam patterned sulfonated SAMs described previously.[29] For solutions at higher pH, however, deposition occurred onto unmodified surfaces as well as sulfonated surfaces after longer induction times. This occurred because the supersaturation was large enough to promote heterogeneous nucleation onto the hydrophobic, higher interfacial energy surfaces.

This indicates that a surface that does not promote nucleation at low supersaturation because of a high interfacial energy may do so at higher supersaturation. The ability to localize deposition as seen in Figure 4 really depends on relative values of ΔG^* and induction time between the two surfaces. These factors can be tuned by varying the supersaturation and relative interfacial energies.

Film Morphology and Phase. Figure 5 shows an FEM tilted view and TEM cross sections of thin film samples. Samples were deposited onto sulfonated polystyrene from pH 2.1, 2×10^{-3} M iron nitrate solutions at 70 °C (Figure 5a) and pH 2, 1×10^{-3} M iron chloride

(28) Abbott, N. L.; Folkers, J. P.; Whitesides, G. M. *Science* **1992**, *257*, 1380.
(29) Rieke, P. C.; Tarasevich, B. J.; Wood, L. L.; Engelhard, M. H.; Baer, D. R.; Fryxell, G. E.; John, C. M.; Laken, D. A.; Jaehnig, M. C. *Langmuir* **1994**, *10*, 619.

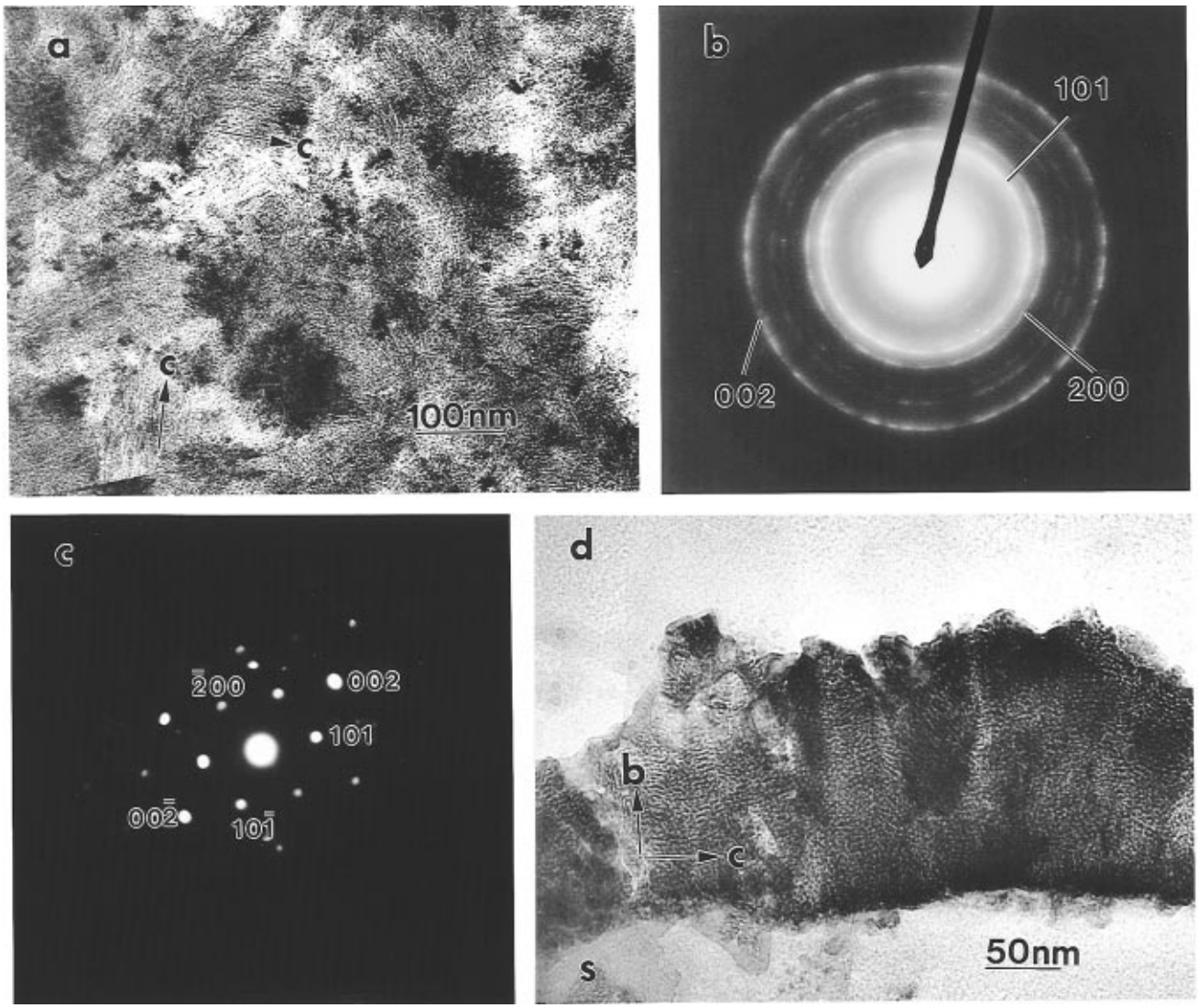

Figure 6. (a) TEM planar view of goethite film, (b) large-area diffraction pattern of planar film, (c) microdiffraction pattern from individual crystallite of planar film, and (d) TEM cross section of goethite film, all showing (020) orientation; s, substrate. Arrows denote crystal axis directions.

solutions at 70 °C (Figure 5b). The film on the sulfonated SAM was deposited from a pH 2, 3×10^{-3} M iron nitrate solution at 70 °C (Figure 5c).

Figures 5a and 5b show continuous films consisting of densely packed crystallites and film thicknesses varying from 0.08 to 0.1 μm. The thickness was limited by the occurrence of solution precipitation which depleted species available for heterogeneous growth. Thicker films were formed (up to 1 μm) using conditions that resulted in no solution precipitation, larger solution volumes, or repeated additions of fresh solution. Such a film is shown in Figure 5c. The dense morphology is similar to that of films deposited by vapor deposition.[18] We attribute the high densities to the heterogeneous nucleation process which allows molecule by molecule growth. This type of growth is more space filling than the packing of solution-formed colloidal particles.

Surface views of films (such as Figures 5a and 6a) show that they consist of individual crystallites. The crystallite nature of the films suggests formation from randomly distributed nuclei that grow and coalesce to form continuous films. FEM cross sections of films indicated that coalescence had occurred by the time the crystallites were ~300−500 Å in diameter. After further deposition times, film growth resulted in thickness increases in the perpendicular direction. Crystallites then consisted of anisotropic columnar structures (e.g. Figure 5c) whose aspect ratio depended on the film thickness. The columns were continuous from substrate to surface indicating that each was associated with one nucleus. There were no significant differences in gross morphologies between films on sulfonated SAMs on silicon and sulfonated polystyrene indicating that deposition is controlled by the sulfonate group−solution interface and not the underlying substrate.

X-ray and electron diffraction analyses indicated that the films in Figures 5a and 5c were goethite (α−FeOOH) and Figure 5b was akaganeite (β−FeOOH). The formation of akaganeite from acidic iron chloride solutions is consistent with results for solution precipitation of particles. Iron chloride complexes (such as $FeCl^{2+}$) form in acidic solutions and stabilize the more soluble akaganeite phase.[30] Goethite films were formed from iron nitrate solutions. The formation of goethite would be expected since solubility line calculations indicated that

(30) Goni-Elizalde, S.; Garcia-Clavel, M.; Tejedor-Tejedor, M. I. *React. Solids* **1987**, *3*, 139.

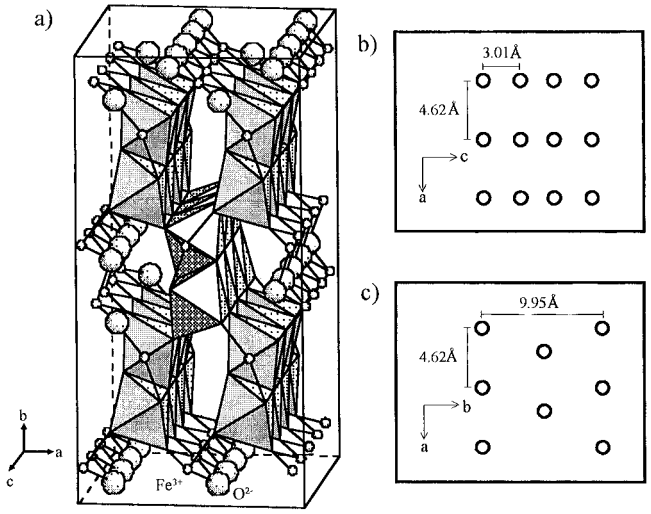

Figure 7. (a) A 3-dimensional schematic drawing of 16 unit cells of goethite with (020) orientation using the *Pbnm* space group. The octhedra consist of central Fe^{3+} cations coordinated to six O^{2-} and/or OH^- anions at the corners, (b) Fe^{3+} cations in the *ac* plane, and (c) Fe^{3+} cations in the *ab* plane.

our solutions were supersaturated with respect to goethite but undersaturated with respect to amorphous phases.

Formation of Oriented Films. Films were deposited at 70 °C from pH 2.1, 2×10^{-3} M iron nitrate solutions onto fully sulfonated polystyrene and planar and cross sections of intact films were obtained by ultramicrotoming epoxy-embedded samples. Figure 6a shows a planar view of a film, Figure 6b shows a large area diffraction pattern of the planar film, Figure 6c shows a microdiffraction pattern of a single crystallite of the planar film, and Figure 6d shows a cross section of the film. The microdiffraction pattern is representative of several crystallites randomly sampled on the film. The diffraction rings and spots correspond to reflections of goethite. Primarily {101}, {002}, and {200} reflections are present indicating a high degree of "*b*"-axis orientation perpendicular to the substrate using an orthorhombic unit cell with *Pbnm* space group and $a_0 = 4.62$ Å, $b_0 = 9.95$ Å, and $c_0 = 3.01$ Å. This indicates that growth occurs from "*ac*" planes such as the (020) plane. This orientation is shown schematically in Figure 7a. Figure 7a shows that the "*c*" or [001] axis is oriented parallel to the substrate. This axis corresponds to the direction of double chains of edge-shared octahedra with Fe−Fe spacings of 3.01 Å. The ring pattern was obtained from an area containing many crystallites and indicates that although one crystallite axis is oriented with respect to the substrate, the (020) planes of adjacent crystallites are not oriented with respect to each other. This results in polycrystalline oriented films.

Similar crystallite orientations occurred for heterogeneous nucleation of akaganeite films from iron chloride solutions and for films deposited onto sulfonated SAMs. The akaganeite orientation also resulted in the [001] axis parallel to the substrate. Akaganeite is similar to goethite in that double chains of edge-shared octahedra form along the [001] direction but adjacent chains are connected by corner sharing in a more open arrangement.

The (020) orientation with chains of octahedra running parallel to the substrate is also indicated by visual examination of micrographs. The planar view in Figure 6a and the cross section in Figure 6d show that the crystallites have substructures consisting of chains or laths running parallel to the substrate. These structures are well-known in goethite particles as [001] chains.[31] Several regions in the cross section in Figure 6d show crystallites with successive layers of chains. Each lath is 20−30 Å in the "*b*" direction which corresponds to three or four double chains of edge-shared octahedra. This morphology indicates that growth in the "b" or perpendicular direction occurs by the layer-by-layer growth of chains in the "*c*" direction. Chains grow laterally until they coalesce with chains from adjacent crystallites. This type of growth may be promoted by the relatively high rate of growth in the "*c*" direction and the polymerization-type hydrolysis and condensation reactions found in iron hydroxide systems.

There are two faint rings in Figure 6b corresponding to planes slightly off axis from the "*b*" axis. These occurred due to slightly misoriented crystallites at larger distances away from the substrate or damage during sample preparation. The strong diffraction rings and spots and well developed lath substructures observed in numerous samples, however, indicate that the primary orientation is (020).

The cross-section micrographs in Figure 5 show development of triangular faces at the solution interface with obtuse angles of ∼120° for both the 0.08 and 0.4 μm films. These faces were not examined by diffraction, but the geometry shows that they are higher index planes. The triangular morphology reflects the layer-by-layer growth mechanism with growth initiating at the center of each crystallite and proceeding laterally until coalescence occurs with adjacent crystallites. This morphology is quite different than the morphology of goethite particles formed by homogeneous precipitation. These particles consist of needles elongated along the [001] direction with well-developed (100) and (010) faces.[31]

Goethite has been found to grow with similar orientations as our films in biomineralized tissue of limpet teeth. Mann et al. found that the [001] direction is oriented parallel to fibers of the organic matrix.[32] They suggested that spatial constraints imposed by the fibers and possible chemical interactions between growing mineral and organic fiber controlled this orientation.

It is not clear what causes the [001] orientation in our 2-d organic interface/inorganic thin film system. It is difficult to explain the orientation in terms of epitaxial spatial relationships between sulfonate sites and the goethite crystal lattice. The (020) or "*ac*" planes consist of iron cations with spacings of 3.01 and 4.62 Å as shown in Figure 7b. This plane has the densest packing of iron cations compared to other planes such as the "*ab*" plane shown in Figure 7c. The sulfonate sites are spaced at ∼5 Å. This indicates that spatial matching would be possible in the "*a*" direction but not the "*c*" direction. We found that iron species adsorbed onto sulfonate sites resulting in Fe/S ratios of ∼0.4 by XPS. This indicates that one $FeOH^{2+}$ species is coordinated with ∼2 sulfonate sites to preserve electroneutrality. This would

(31) Atkinson, R. J.; Posner, A. M.; Quirk, J. P. *J. Inorg. Nucl. Chem.* **1968**, *30*, 2371.
(32) Mann, S.; Perry, C. C.; Webb, J.; Luke, B.; Williams, R. J. P. *Proc. R. Soc. London B* **1986**, *227*, 179.

result in average adsorbed iron species intersite spacings even greater than the 5 Å sulfonate intersite spacing. The interactions that control orientation may be less specific than strict spatial relationships between surface sites and solution species. A better understanding of how the organic interfaces control orientation will require further understanding of iron species−sulfonate site interactions and iron hydroxide deposit structure in the initial stages of growth.

The sulfonate sites are disordered in the polystyrene system. (The structure of the SAM interface is not known.) This indicates that it is not necessary to have ordered organic lattices to obtain oriented inorganic structures, at least with one axis oriented with respect to the substrate. This was also suggested by calcium carbonate growth onto sulfonated polystyrene[1] and liquid-phase Langmuir monolayers[2] where some degree of inorganic perpendicular orientation occurred even with disordered organic structures. Ordered organic lattices, however, can lower the interfacial energy for nucleation and promote nucleation at lower supersaturation values. In addition, the formation of crystallites with all three axes oriented with respect to each other (which would result in multinuclear single crystals upon coalescence) may require organic lattices with long-range order.

Control of iron hydroxide crystal orientation is of much practical interest in magnetic film applications. The most common particulate magnetic tape systems are composed of anisotropic maghemite particles formed by phase conversion of anisotropic goethite particles.[33] The [001] orientation of goethite becomes the [011] direction of maghemite and this is the magnetization direction of maghemite. Colloidal suspensions of crystallites in a binder are aligned in a magnetic field with [011] directions parallel to the substrate resulting in ∼30−40 vol% films with longitudinal magnetization. Our studies resulted in the direct growth of denser films of crystallites oriented parallel to the surface. Work has been done to completely convert the films to oriented maghemite.[34] This suggests that our films may be of interest for high-density magnetic storage devices.

Summary

We have demonstrated that iron hydroxide thin films can be grown onto sulfonated polystyrene and sulfonated SAMs on silicon from solution. The deposition mechanism depended on the solution supersaturation which was controlled by varying the pH and temperature. Deposition occurred by heterogeneous nucleation at a specific range of supersaturation values just below the critical supersaturation, resulting in the formation of dense, continuous films. These films were similar in appearance to vapor-deposited films, only from aqueous solutions at lower temperatures. Solution precipitation occurred at higher supersaturation values (above pH 3) and films formed by adsorption of colloidal particles resulting in less dense and less adherent films.

The sulfonate sites had a significant effect in promoting heterogeneous nucleation and growth compared to hydrophobic surfaces. This was used to localize deposition to form patterned films onto substrates patterned with sulfonate sites. Induction times decreased with increasing sulfonate site density due to a reduction in interfacial energy.

Films formed by the growth of randomly distributed nuclei that coalesced to form continuous films. After coalescence, film growth continued in the perpendicular direction to form columnar crystallites. Each crystallite consisted of successive layers of 20−30 Å thick chain substructures indicating that growth in the perpendicular direction occurred by layer-by-layer growth in the lateral direction after coalescence. A high degree of (020) orientation occurred for goethite and akaganeite resulting in the [001] or chain direction parallel to the substrate.

There are many other questions to be answered concerning the mechanisms of nucleation and growth. It would be interesting to further examine the effects of site density and structure on nucleation rate in order to see whether the interfacial energy can be tailored by systematically varying the organic site properties. Other issues include how cations are adsorbed and arranged relative to surface sites, how orientation is controlled, and how microstructures evolve from nuclei to coalesced films. In addition, our studies have involved nucleation and growth onto sulfonated surfaces exclusively. We have done initial studies that indicate iron hydroxide can be deposited onto carboxylic acid groups on polyethylene and carboxylic acid-terminated alkyl thiols on gold. The interfacial energy may vary with functional group and affect the kinetics of nucleation and growth as well as the orientation. This work suggests it should be possible to deposit other materials by heterogeneous nucleation from solution onto organic interfaces and by an understanding of how to control the solution and interfacial chemistry.

Acknowledgment. This work was supported by the U.S. Department of Energy, Office of Basic Energy Sciences, under Contract DE-AC06-76RLO 1830. The authors are grateful to P. Bush at the University of Buffalo for obtaining the FEM micrograph and B. Bunker for a critical review of the manuscript.

CM940391E

(33) Sharrock, M. P. *IEEE Trans. Magn.* **1989**, *25*, 4374.

(34) Bunker, B.; Rieke, P. C.; Tarasevich, B. J.; Campbell, A. A.; Fryxell, G. E.; Graff, G. L.; Song, L.; Liu, J.; Virden, J. W.; McVay, G. L. *Science* **1994**, *264*, 48.